

MOL Solvers for Hyperbolic PDEs with Source Terms.

I. Ahmad and M. Berzins

School of Computer Studies, The University of Leeds, Leeds LS2 9JT, UK.

Abstract

A method-of-lines solution algorithm for reacting flow problems modelled by hyperbolic p.d.e.s with stiff source terms is presented. Monotonicity preserving advection schemes are combined with space/time error balancing and a Gauss-Seidel iteration to provide an efficient solver. Numerical experiments on two challenging examples are presented to illustrate the performance of the method.

1 Introduction

A currently active area of research is the numerical solution of hyperbolic partial differential equations (p.d.e.s) with stiff non-linear source terms [9,11]. Tang [11] and others have concentrated on the convergence while Papalexandris et al. [9] and others (e.g. Leveque) have considered new spatial discretization methods. The difficulty of solving such problems was illustrated by [8] who showed that spurious numerical solution phenomena, such as incorrect wave speeds may occur when insufficient spatial and temporal resolution are used.

In this paper the application of the method of lines to such problems is considered. Monotone spatial discretization schemes are used to reduce the PDE to a system of ordinary differential equations (ODEs) in time. For reacting flow problems the spatial mesh points should be chosen with great care to reflect the true solution of the PDE and to avoid generating significant but spurious numerical solution features. One way of achieving this is to use one of the many adaptive mesh algorithms, [3], to control the spatial discretisation error by refining and coarsening the mesh. The aim here is not only to use such algorithms but also to integrate in time with sufficient accuracy so that the spatial error is not degraded while maintaining the efficiency of the time integrator. This has been achieved by varying the time accuracy tolerance with spatial error rather than keeping it fixed thus extending the work of Berzins [3] to problems with stiff source terms. Such problems require the

use of implicit methods to resolve the fast transients associated with some chemistry species. For problems involving many species the cost of using implicit methods may be high unless great care is taken with numerical linear algebra. In the present work this is done by making use of a method developed for method of lines solvers applied to atmospheric chemistry problems, [13,2]. The approach uses a Gauss-Seidel iteration applied to the source terms alone. The advective terms are effectively treated explicitly but without introducing a splitting error. The first part of this paper deals with the implementation of these ideas for a 1D hyperbolic conservation law with a nonlinear source term, [8], while the second part will show results for the more complex problem of Fedkiw [6,7].

2 Spatial Discretisation and Time Integration

The 1D Leveque and Yee problem [8], is given by

$$\frac{\partial u}{\partial t} + \frac{\partial u}{\partial x} = -\psi(u) \quad x \in [0, \infty), \quad \psi(u) = \mu u(u-1)(u-0.5) \quad (1)$$

and is the linear advection with a source term that is "stiff" for large μ . The initial and boundary values (at $x = 0$) are defined by

$$u(x, 0) = u_0(x) = u_L = 1, x \leq x_d; \quad u_R = 0, x > x_d$$

where $x_d = 0.1$ or 0.3 in the cases considered here. The infinite domain will also be truncated to $[0, 1]$ for the cases considered here, as this is sufficient to demonstrate the behaviour of the methods employed. A simple outflow boundary condition is then used at $x = 1$. The solution of equation (1) is a discontinuity moving with constant speed and has a potentially large source term that only becomes active at the discontinuity, [8].

Defining a spatial mesh $0 = x_1 < \dots < x_N = 1$ and the vector of values \mathbf{U} with components $U_i(t) \approx u(x_i, t)$ where $u(x, t)$ is the exact solution to the p.d.e. and $U_i(t)$ is the exact solution to the o.d.e. system derived by spatial semi-discretization of the p.d.e. and given by

$$\dot{\mathbf{U}} = \mathbf{F}_N(t, \mathbf{U}(t)), \quad \mathbf{U}(0) \text{ given}, \quad (2)$$

and this true solution $[\mathbf{U}(t_n)]_{n=0}^p$ is approximated by $[\mathbf{V}(t_n)]_{n=0}^p$ at set of discrete time $0 = t_0 < t_1 < \dots < t_p = t_e$ by the time integrator. The form of the ODEs system given by equation (2) at time t is given by

$$\mathbf{F}_N(t_n, \mathbf{U}(t_n)) = \mathbf{F}_N^f(t_n, \mathbf{U}(t_n)) + \mathbf{F}_N^s(t_n, \mathbf{U}(t_n)). \quad (3)$$

where the vector $\mathbf{F}_N^f(t_n, \mathbf{U}(t_n))$ is the second-order limited discretisation of the advective terms in equation (1) whose components are given by

$$F_j^f(t, \mathbf{U}(t)) = - \left[1 + \frac{B(r_j, 1)}{2} - \frac{B(r_{j-1}, 1)}{2r_{j-1}} \right] \frac{(U_j(t) - U_{j-1}(t))}{\Delta x} \quad (4)$$

where B is a limiter such as that of van Leer: (see [3])

$$B(r_j, 1) = \frac{r_j + |r_j|}{1 + r_j}, \text{ and } r_j = \frac{U_{j+1}(t) - U_j(t)}{U_j(t) - U_{j-1}(t)}. \quad (5)$$

The vector $\mathbf{F}_N^s(t, \mathbf{U}(t))$ represents the approximate spatial integration of the source term which is defined by $\frac{1}{\Delta x} \int_{x_{j-\frac{1}{2}}}^{x_{j+\frac{1}{2}}} \psi(U(x, t)) dx$ and is evaluated by using the midpoint quadrature rule so that its j th component is:

$$F_j^s(t, U_j(t)) = \psi(U_j(t)). \quad (6)$$

The time integration method used here (mostly for simplicity of analysis) is the Backward Euler method defined by

$$\mathbf{V}(t_{n+1}) = \mathbf{V}(t_n) + \mathbf{F}_N(t_{n+1}, \mathbf{V}(t_{n+1})). \quad (7)$$

In the case when a modified Newton method is used to solve the nonlinear equations at each timestep, this constitutes the major computational task of a method of lines calculation. In cases where large o.d.e. systems that result from the discretization of the flow problems with many chemistry species the c.p.u. times may be excessive unless special iterative methods are used.

The approach taken here follows [4] in neglecting the advective terms $J_f = \frac{\partial \mathbf{F}^f}{\partial \mathbf{V}}$, and concentrates on the Jacobian of the source terms $J_s = \frac{\partial \mathbf{F}^s}{\partial \mathbf{V}}$ when forming the Jacobian matrix used in the Newton iteration. This approach, in the case when no source terms are present, corresponds to using functional iteration for the advective calculation, see [2,4]. The matrix $I - \Delta t \gamma J_s$ is the Jacobian matrix of that part of the o.d.e. system corresponding to the discretization of the time derivatives and the source terms. This matrix is thus block-diagonal with as many blocks as there are spatial elements and with each block having as many rows and columns as there are p.d.e.s. The fact that a single block relates only to the chemistry within one cell means that each block's equations may be solved independently by using a Gauss-Seidel iteration, which has also been used with great success for atmospheric chemistry problems, [13]. The nonlinear equations iteration employed here may thus be written as

$$[I - \Delta t J_s] [\mathbf{V}^{m+1}(t_{n+1}) - \mathbf{V}^m(t_{n+1})] = \mathbf{r} \left(t_{n+1}^m \right) \quad (8)$$

where $\mathbf{r}(t_{n+1}^m) = -\mathbf{V}^m(t_{n+1}) + \mathbf{V}(t_n) + \Delta t \mathbf{F}_N(t_{n+1}, \mathbf{V}^m(t_{n+1}))$. This approximation is only used to speed up the solution of the nonlinear equations and, providing that the iteration converges, has no adverse impact on accuracy. In order for this iteration to converge with a rate of convergence r_c it is necessary, [2], that

$$\| [I - \Delta t J_s]^{-1} \Delta t J_f \| = r_c \quad \text{where } r_c < 1. \quad (9)$$

Using the identity $\| ab \| \leq \| a \| \| b \|$, and noting that J_f may be written as $(\Delta x)^{-1} J_f^*$ gives:

$$\frac{\Delta t}{\Delta x} \| J_f^* \| \leq r_c \| [I - \Delta t J_s] \| . \quad (10)$$

For the p.d.e. in (1), $[I - \Delta t J_s]$ is a diagonal matrix with entries $1 + \Delta t \mu \frac{\partial \psi}{\partial V}$ where

$$\frac{\partial \psi}{\partial V} = p(V) \quad (11)$$

and where $p(V) = 3V^2 - 3V + 0.5$ gives a CFL type condition that allows larger timesteps as μ increases. The function $p(V)$ is bounded between the values 0.5 and -0.25 for solution values in the range $[0, 1]$.

3 Space-Time Error Balancing Control.

Hyperbolic PDEs are often solved by using a CFL condition to select the timestep. One alternative approach developed by Berzins [3,4] is to use a local error per unit step control in which the time local error (denoted by $\mathbf{le}(t)$) is controlled so as to be smaller than by the local growth in the spatial error over the timestep (denoted by $\mathbf{est}(t)$). In the case of the Backward Euler method the standard local error estimate at t_{n+1} is defined as $\mathbf{le}(t_{n+1})$ and is estimated in standard ODE codes by

$$\begin{aligned} \mathbf{le}(t_{n+1}) &= \frac{\Delta t}{2} [\mathbf{F}_N(t_{n+1}, \mathbf{V}(t_{n+1})) - \mathbf{F}_N(t_n, \mathbf{V}(t_n))] . \\ &\approx \frac{\Delta t^2}{2} \ddot{\mathbf{V}}(t_{n+1}) \end{aligned} \quad (12)$$

The error control of [3] is defined by

$$\| \mathbf{le}_{n+1}(t_{n+1}) \| \leq \epsilon \| \mathbf{est}(t_{n+1}) \| \quad (13)$$

where $0 < \epsilon < 1$ is a balancing factor and $\mathbf{est}(t_{n+1})$ represents the local growth in time of the spatial discretisation error from t_n to t_{n+1} , assuming that the error is zero at t_n . Once the primary solution has been computed using the method of Section 2, a secondary solution is estimated at same time step with an upwind scheme of different order and a different quadrature rule for source term integration. The difference of these two computed solution is then taken as an estimate of the local growth in time of the spatial discretization error in the same way as in [3]. The primary solution $\mathbf{V}(t_{n+1})$ starting from $\mathbf{V}(t_n)$ is computed in the standard way as described in Section 2. The secondary solution $\mathbf{W}(t_{n+1})$ is computed by solving

$$\dot{\mathbf{W}}(t) = \mathbf{G}^f(t, \mathbf{W}(t)) + \mathbf{G}^s(t, \mathbf{W}(t)), \quad \mathbf{W}(t_n) = \mathbf{V}(t_n). \quad (14)$$

with initial value \mathbf{V}_n , where \mathbf{G}^f and \mathbf{G}^s are the first order advective term and the source terms which are evaluated using a linear approximation on each interval and the trapezoidal rule i.e.

$$\begin{aligned} G_j^f(t, W_j(t)) &= -\frac{(W_j(t) - W_{j-1}(t))}{\Delta x}, \\ G_j^s(t, W_j(t)) &= \frac{1}{4}(\psi(W_{j-1}(t)) + 2\psi(W_j(t)) + \psi(W_{j+1}(t))). \end{aligned} \quad (15)$$

Estimating $\mathbf{es}(t_{n+1})$ by applying the Backward Euler Method to (14) subtracted from (7) with one iteration of the modified Newton iteration of the previous section, as in [4], gives

$$\begin{aligned} [I - \Delta t J_s][\mathbf{es}(t_{n+1})] &= \Delta t [\mathbf{F}^f(t_{n+1}, \mathbf{V}(t_{n+1})) - \mathbf{G}^f(t_{n+1}, \mathbf{V}(t_{n+1})) \\ &\quad + \mathbf{F}^s(t_{n+1}, \mathbf{V}(t_{n+1})) - \mathbf{G}^s(t_{n+1}, \mathbf{V}(t_{n+1}))] \end{aligned} \quad (16)$$

where $\mathbf{es}(t_{n+1}) \approx \mathbf{V}(t_{n+1}) - \mathbf{W}(t_{n+1})$. From this the estimate of the local growth in time of the spatial discretization error and is given at the j th grid point by

$$\begin{aligned} &[1 + \Delta t \mu_p(V_j(t_{n+1}))]est_j(t_{n+1}) \\ &= \frac{\Delta t}{2\Delta x} [B(\tilde{r}_j, 1) - \frac{1}{\tilde{r}_{j-1}} B(\tilde{r}_{j-1}, 1)] (V_j(t_{n+1}) - V_{j-1}(t_{n+1})) \\ &\quad + \frac{\Delta t}{4} (\psi(V_{j-1}(t_{n+1})) - 2\psi(V_j(t_{n+1})) + \psi(V_{j+1}(t_{n+1}))). \end{aligned} \quad (17)$$

where $p(V)$ is defined as in equation(10) and $\tilde{r}_j = \frac{V_{j+1}(t) - V_j(t)}{V_j(t) - V_{j-1}(t)}$. The term involving the limiter $B(.,.)$ may be rewritten as in [3], equation (5.13), as:

$$[B(\tilde{r}_j, 1) - \frac{1}{\tilde{r}_{j-1}}B(\tilde{r}_{j-1}, 1)](V_j(t_{n+1}) - V_{j-1}(t_{n+1})) = [\alpha_j V_{j,xx}^{n+1} + \beta_j V_{j-1,xx}^{n+1}]. \quad (18)$$

where α_j and β_j are both in the range $[0, 1]$ and where $V_{j,xx}^{n+1} = V_{j+1}(t_{n+1}) - 2V_j(t_{n+1}) + V_{j-1}(t_{n+1})$ and $V_{j-1,xx}^{n+1}$ is similarly defined. Hence

$$(\psi(V_{j-1}(t_{n+1})) - 2\psi(V_j(t_{n+1})) + \psi(V_{j+1}(t_{n+1}))) \approx p(V_i) V_{j,xx}^{n+1},$$

where $p(V)$ is defined by equation (11), then gives $est_j(t_{n+1})$ as

$$[1 + \Delta t \mu p(V_j(t_{n+1}))] est_j(t_{n+1}) \approx \frac{\Delta t}{\Delta x} [\alpha_j V_{j,xx}^{n+1} + \beta_j V_{j-1,xx}^{n+1}] + \frac{\Delta t}{4\Delta x^2} p(V_i) V_{j,xx}^{n+1}, \quad (19)$$

Let $V_{j,xx}^* = \max(V_{j,xx}^{n+1}, V_{j-1,xx}^{n+1})/\Delta x^2$ and then rewrite this equation as

$$|est_j(t_{n+1})| \leq \frac{\Delta t \Delta x |\alpha_j + \beta_j + \mu \Delta x p(V_j(t_{n+1})/4|}{|1 + \Delta t \mu p(V_j(t_{n+1}))|} |V_{j,xx}^*|$$

and define the vector $\mathbf{E}(x, V, t)$ as having components $E_j(x, V_j, t)$ where

$$E_j(x, V_j, t) = \frac{|2 + \mu \Delta x p(V_j(t_{n+1})/4|}{|1 + \mu \Delta t p(V_j(t_{n+1}))|}.$$

Taking norms after defining the vector \mathbf{V}_{xx}^* as having components $V_{j,xx}^*$, gives

$$\| \mathbf{est}(t_{n+1}) \| \leq \Delta x \Delta t \| \mathbf{E}(x, V, t) \| \| \mathbf{V}_{xx}^* \|.$$

Combining this equation with (12) shows that another CFL type condition is inherent in the error control defined by (13):

$$\frac{\Delta t}{\Delta x} \leq 2 \epsilon \frac{\| \mathbf{E}(x, V, t) \| \| \mathbf{V}_{xx}^* \|}{\| \mathbf{V}(t_{n+1}) \|} \quad (20)$$

4 Numerical Solution with Fixed Meshes

In initial fixed mesh experiments with the problem defined by equation (1) comparisons were made between the standard local error control approach

in which absolute and relative tolerances RTOL and ATOL are defined, see Pennington and Berzins, [10], and the new approach defined by (13). The choice of the parameter ϵ is an important factor in the performance of the second approach. In selecting this parameter the local growth in the spatial discretization error should dominate the temporal error and the work needed should not be excessive. Obviously the larger the value of ϵ the fewer ODE time steps there will be, and the smaller the value of ϵ the more steps there will be. A good compromise between efficiency and accuracy is to use ϵ in the range 0.1 to 0.3. The numerical experiments described by Ahmad [1] confirm the results of Berzins [3] although it is noted that for some combustion problems, ϵ may have to be reduced below 0.1.

An important feature of solving the problem defined by equation (1) is that the numerical solution may move with an incorrect wave speed. Leveque and Yee [8] showed that the step size and the mesh size should be $O(\frac{1}{\mu})$, to avoid spurious solutions being generated. In order to illustrate these results we have taken $x_d = 0.3$ in equation (1), $\Delta x = 0.02$ and used a fixed time step $\Delta t = 0.015$. The product of time step Δt and the reaction rate μ determines the stiffness of the system. Figure(1) shows the comparison of the computed solution and exact solution at $t = 0.3$ for $\mu = 100$, and 1000 ($\Delta t\mu = 1.5$ and 15) respectively. It is evident from Figure (1) that for smaller $\Delta t\mu$ the strategy

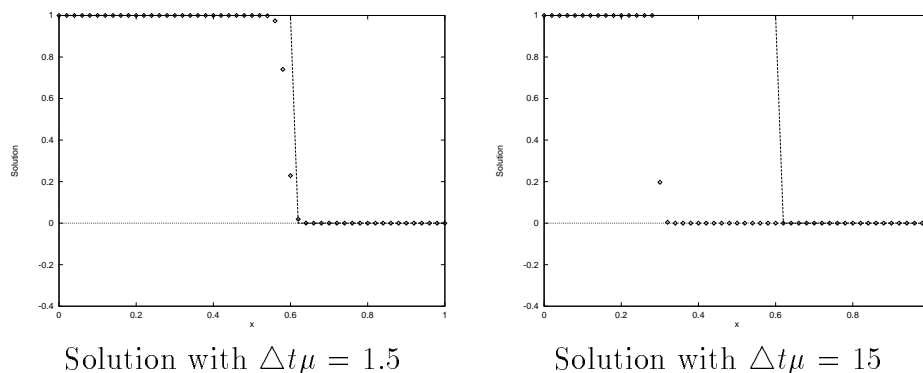


Fig. 1. Comparison of True Solution(line) and Num. Solution(dots) using local error control with 0.01 relative tolerance and 1×10^{-5} absolute tolerance

works well and good results are obtained. But when $\Delta t\mu = 15$, the discontinuity has stopped at $x = 0.3$ and when a trapezoidal quadrature rule was used for the source term, a large undershoot and overshoot occurred in the numerical solution.

5 Local Grid Refinement

In the previous section it was shown that the front is moving with the wrong speed, due to lack of proper spatial resolution. Leveque and Yees [8] pointed out that the source of difficulty is the discontinuity in the solution and that a much finer grid is needed there. One solution, suggested by [8] to such problems is to deploy a method that is capable of essentially increasing the spatial resolution rather than excessive refinement of the overall grid.

For this purpose a monitor function was used to guide the decision where to refine or coarsen the mesh. A commonly used monitor function is the second spatial derivative which however tends to infinity around a shock [10] as the mesh is refined. In order to overcome this we have introduced a new monitor function based upon the local growth in time spatial error \mathbf{est} as defined by equation (13). This leads to the use of local grid refinement, and with the help of the error balancing approach described in Section 3 it is possible to create a new refined grid directly surrounding of the location of the source. For this purpose we have modified the approach described by Pennington and Berzins [10]. The remesh routine bisects the mesh cell if the monitor function is too large or combines two cells into one if the monitor function is well below the required value. In the experiments here remeshing routine is called on every second time step. The adaptive mesh initially starts with 26 points and when the error was larger than specified limit then the corresponding cell is subdivided into two with a 75 maximum points being allowed for the case shown in Figure 2, which shows the front moving correctly.

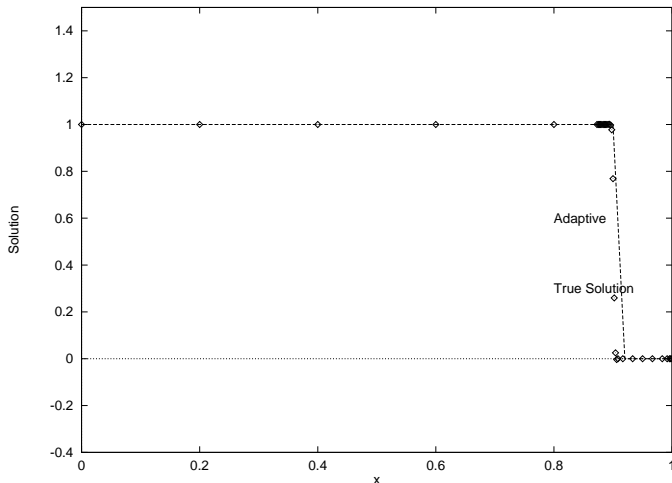


Fig. 2. Comparison of True Solution (lines) and Computed Solution(Dots) with grid refinement technique at time equal to 0.6.

6 Combustion Problem

Modelling reactive flow in combustion problems is based on a generally accepted set of time-dependent coupled partial differential equations maintaining conservation of density, momentum and energy. There are basically four types of physical processes represented in reactive flow equations. These processes are chemical reactions, diffusive transport, convection and wavelike properties, [6]. The chemical kinetics represents the production and loss of the chemical species, convection describes the motion of fluid quantities in space. The wave-like behaviour are described implicitly in the reactive flow equations by the coupled continuity equations. The important point about wavelike motion is that energy is transferred from one element of the fluid to others by waves that can travel much faster than the fluid velocity.

The main type of wave considered here is a shock wave, which moves as a discontinuity through the domain. The shock wave heats and compresses the undistributed reactive mixture as it passes through it. The raised temperature triggers chemical reactions; energy release eventually occurs and the pressure waves are generated, some of which propagate forward and accelerate the shock wave. The reactions may proceed very rapidly after the initiation, which will make the source term stiff [12,13] in time, hence it is possible that the solution will yield non-physical waves with incorrect speed and incorrect discontinuous in flow properties [6,12].

The governing equations of the combustion problem considered here are the Euler equations modified in such a way that the flow of more than one species can be considered, Ton et al. [12] and Fedkiw [6]:

$$\mathbf{u}_t + [\mathbf{f}(\mathbf{u})]_x = \psi(\mathbf{u}), \quad (21)$$

where

$$\mathbf{u} = \begin{bmatrix} \rho \\ \rho u \\ E \\ \rho Y_1 \\ \vdots \\ \rho Y_{NS-1} \end{bmatrix} \quad \mathbf{f}(\mathbf{u}) = \begin{bmatrix} \rho u \\ \rho u^2 + p \\ (E + p)u \\ \rho u Y_1 \\ \vdots \\ \rho u Y_{NS-1} \end{bmatrix} \quad \psi(\mathbf{u}) = \begin{bmatrix} 0 \\ 0 \\ 0 \\ \dot{w}_1(T, p, Y_1, \dots, Y_{NS-1}) \\ \vdots \\ \dot{w}_{NS-1}(T, p, Y_1, \dots, Y_{NS-1}) \end{bmatrix}$$

and \dot{w}_i represents the mass production rate of the i th species and where the

energy equation is given by

$$E = -p + \frac{\rho u^2}{2} + \rho h, \quad (22)$$

where h is the enthalpy. NS represents the number of species (nine in all) and Y_i is the mass fraction of species i and $Y_{NS} = 1 - \sum_{i=1}^{NS-1} Y_i$. The equation of state for the mixture of gas is given by $p = \rho \left[\sum_{i=1}^{NS} Y_i R_i \right] T$.

In this one-dimensional shock tube test problem with chemistry, as given in [1,6,7], a shock hits a solid wall boundary and is reflected. Then, after a delay, a reaction wave kicks in at the boundary. The reaction wave eventually merges with the shock causing a split into 3 waves. From wall to outflow (left to right) these waves are a rarefaction, a contact discontinuity and a shock (see Fedkiw [6,7]). Following Fedkiw [6,7] we have taken 2/1/7 molar ratio of H₂/O₂/Ar and all the gases are assumed to be thermally perfect with initial data values

$$\rho = .072 \frac{kg}{m^3}, \quad u = 0 \frac{m}{s}, \quad p = 7173 \frac{J}{m^3}, \quad (23)$$

on the left and on the right the initial data is given by

$$\rho = .1870 \frac{kg}{m^3} \quad u = -487.34 \frac{m}{s}, \quad p = 35594 \frac{J}{m^3}, \quad (24)$$

The length of domain is 10cm and time is 230 μ s. The left side boundary conditions are reflective, while transmissive boundary conditions have been implemented on right hand side of the domain. The domain has been discretized into 400 equally spaced grid cells. To handle the steep spatial fronts, it is natural to apply modern shock-capturing numerical methods for the convective terms. The spatial discretization method was that of Section 2 combined with the Marquina flux method [5] whose excellent shock-capturing behaviour on non-reacting flows, has motivated its use here for reacting flow. The theta method, [3], together with Gauss Seidel iterative method has been used for the time integration. Thus the methods used are somewhat different to the ENO approach adopted in Fedkiw[6,7]. For full details see Ahmad [1].

The results obtained from the code are not entirely oscillation free - there is small oscillation due to fact the numerical method has to resolve a one cell thick shock. For many of the chemistry components the solution values in all cases were very similar. Substantial differences were observed in the H₂O₂ and HO₂ species and these are displayed from left to right as cases A,B and C in Figures 3 and 4. The results with new error control strategy given by equation (13) are given in Figures (3,4) as case A. For time of 230 μ s and the code took 6532 steps and the results are comparable to Fedkiw[6,7]. The code has also

been run with a standard local error per step control strategy as given by equation with different relative (RTOL) and absolute (ATOL) values. With $RTOL=0.1$ and $ATOL=1 \times 10^{-4}$, in this case, the code halted after some time due to negative pressure being generated near the boundary and consequently a slightly tighter tolerance has been used and the code has been run with $RTOL=0.1$ and $ATOL=10^{-5}$. In this case the code took 5549 steps to reach the final time= $230\mu s$ and got small oscillations as given in case B of Figures (3,4). When the code was run with $RTOL=0.01$ and $ATOL=10^{-5}$, the code took 8207 steps and the results are given as case C in Figures (3,4). Again small oscillations are visible in this case.

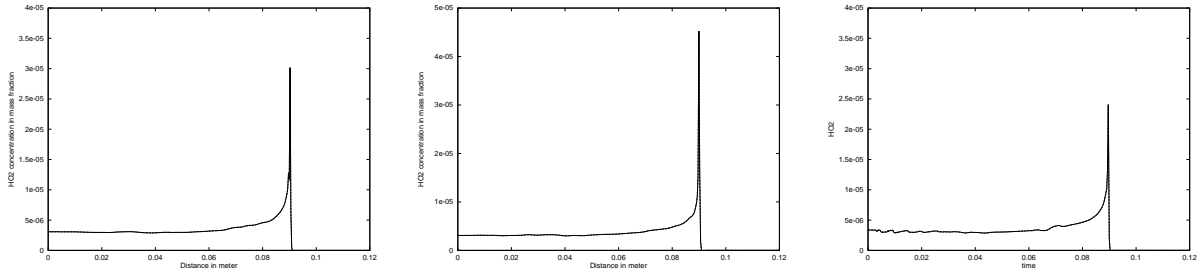


Fig. 3. Cases A,B,C: H_2O_2 Component Values at time= $230\mu s$.

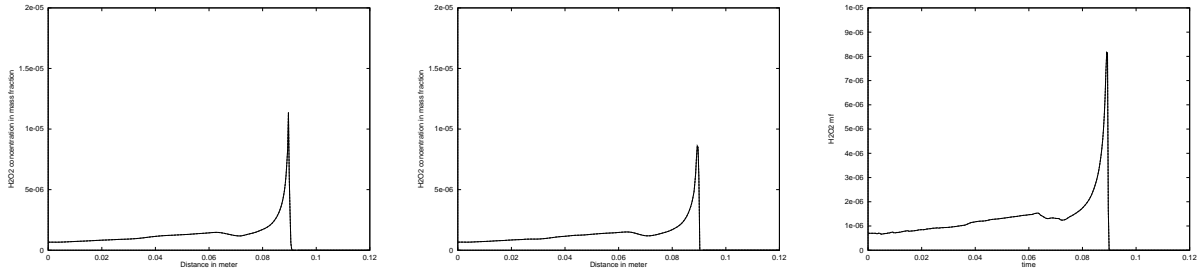


Fig. 4. Cases A,B,C: H_2O_2 Component Values at time= $230\mu s$.

With both strategies, the results are of comparable accuracy except for the species HO_2 and H_2O_2 . When the LEPS strategy is being used, a comparison of results with Fedkiw [6,7] shows that for 0.1 relative tolerance the HO_2 peak is higher and the H_2O_2 peak is smaller while for 0.01 relative tolerance the HO_2 peak is comparable to Fedkiw [6] but the peak of H_2O_2 is smaller. On the other hand when LEPUS strategy is being used HO_2 is identical to Fedkiw [6] and H_2O_2 is only slightly smaller than Fedkiw [6,7]. From this we again draw the conclusion that LEPUS control strategy gives solution with the comparable accuracy to that of the LEPS control strategy, but for this extremely stiff and nonlinear problem, there is a need to reduce the balancing factor ϵ to 0.025.

Acknowledgements

IA would like to thank the Pakistan Government for Ph.D studentship support and Dr R. Fedkiw for his help with the combustion model formulation.

References

- [1] I. Ahmad. The Numerical Solution of Reacting Flow Problems. Ph.D Thesis, School of Computer Studies, University of Leeds, 1999.
- [2] I. Ahmad and M. Berzins. An algorithm for ODEs from atmospheric dispersion problems. *Applied Numerical Mathematics*, 25:137–149, 1997.
- [3] M. Berzins. Temporal error control for convection-dominated equations in two space dimensions. *SIAM Journal on Scientific and Statistical Computing*, 16:558–580, 1995.
- [4] M. Berzins and J. M. Ware. Solving convection and convection reaction problems using the M.O.L. *Applied Numerical Mathematics*, 20:83–99, 1996.
- [5] R. Donat and A. Marquina. Capturing shock reflections: An improved flux formula. *Journal of Computational Physics*, 125:42–58., 1996.
- [6] R. P. Fedkiw. *A Survey of Chemically Reacting, Compressible Flow*. UCLA (Ph.D. Dissertation), 1966.
- [7] R. P. Fedkiw, B. Merriman, and S. Osher. High Accuracy Numerical Methods for Thermally Perfect Gas Flows with Chemistry. *Journal of Computational Physics*, 132:175–190, 1997.
- [8] R. J. Leveque and H.C. Yee. A study of numerical methods for hyperbolic conservation laws with stiff source terms. *Journal of Computational Physics*, 86:187–210, 1990.
- [9] M. V. Papalexandris, A. Leonard, and P. E. Dimotakis. Unsplit schemes for hyperbolic conservation laws with source terms in one space dimension. *Journal of Computational Physics*, 134:31–61, 1997.
- [10] S. V. Pennington and M. Berzins. New NAG library software for first-order partial differential equations. *ACM Transactions on Mathematical Software*, 20:63–99, 1994.
- [11] T. Tang. Convergence analysis for operator splitting method applied to conservation laws with stiff source terms. *SIAM Journal on Numerical Analysis*, 35(5):1939–1968, October 1998.
- [12] V. T. Ton, A. R. Karagozian, F. E. Marble, S. J. Osher, and B. E. Engquist. Numerical simulation of high speed chemically reacting flow. *Theoret. Comput. Fluid Dynamics*, 6:161–179, 1994.
- [13] J.G. Verwer. Gauss-Seidel iteration for stiff odes from chemical kinetics. *SIAM Journal on Scientific Computing*, 15:1243–1250, 1994.